Journal of
NANOSTRUCTURES
JNS
NANOSTRUCTURES
JNS.kashanu.ac.ir

A Simple Method for Synthesis of Strontium Ferrite Nanoparticles and their Polymeric Nanocomposites

G. Nabiyouni[a*], A. Yousofnejad[a], M. Seraj[a], S. Farshad Akhtarianfar[b], D. Ghanbari[b]

[a] *Department of Physics, Faculty of Science, Arak University, Arak 38156-88349, Iran*

[b] *Institute of Nano Science and Nano Technology, University of Kashan, Kashan, P.O. Box 87317-51167, I. R. Iran*

Article history:
Received 13/1/2013
Accepted 28/2/2013
Published online 1/3/2013

Keywords:
Hard magnetic
Nanoparticle
Nanocomposite

**Corresponding author:*
E-mail address:
G-nabiyouni@araku.ac.ir
Phone: +98 861 4173401-5
Fax: +98 861 4173406

Abstract

Hard magnetic $SrFe_{12}O_{19}$ (SrM) nanoparticles were synthesized by a facile sonochemical reaction. The magnetic nanoparticles were then added to acrylonitrile-butadiene-styrene, polystyrene, polycarbonate, and poly sulfone to make magnetic nanocomposites. The magnetic properties of the samples were also investigated using an alternating gradient force magnetometer. The strontium ferrite nanoparticles exhibited ferrimagnetic behaviour at room temperature, with a saturation magnetization of 39 emu/g and a coercivity of 5070 Oe. The distribution of the $SrFe_{12}O_{19}$ nanoparticles into the polymeric matrixes increases the coercivity.

1. Introduction

Hexagonal ferrites such as strontium ferrite have been widely used as the hard magnetic materials for permanent magnets, recording media, absorption of microwave radiation, magneto-optic materials and microwave filters. These materials have a potential application at high frequency range due to their very low electrical conductivity, fairly large magneto-crystalline anisotropy, high Curie temperature, large saturation magnetization, mechanical hardness, excellent chemical stability and low production costs [1-12].

In the last two decades polymer matrix nanocomposites have also been extensively investigated since only a small amount of nanoparticles as additives leads to production of novel high-performance materials with excellent physicochemical properties. Polycarbonate (PC) is an important engineering thermoplastic that possesses several different properties such as clear transparency, high impact strength, dimensional stability, flame resistance, high heat distortion temperature, high impact strength and excellent mechanical properties. PC has been widely applied in many areas, including electric and electronic

devices, automobiles, aviation and spaceflight. Acrylonitrile-butadiene-styrene (ABS) is a thermoplastic polymer that is widely used because of its desirable properties and relatively low cost. ABS is composed of a styrene-acrylonitrile copolymer matrix and a grafted polybutadiene phase, which possesses easy processing, good mechanical properties, thermal stability and improved impact strength [13].

It is well recognized that ultrasonic irradiation causes cavitation in an aqueous medium where the formation, growth and collapse of bubbles occur. Cavitation can generate a temperature of around 5000 ^{0}C and a pressure of over 1800 kPa, which enables many chemical reactions to occur [14]. In this work, we report synthesis of $SrFe_{12}O_{19}$ (SrM) using a sonochemically-assisted reaction. The $SrFe_{12}O_{19}$ nanoparticles were then incorporated into the different polymers. The magnetic properties of SrM nanoparticles and polymer/SrM nanocomposites were compared.

2. Experimental

2. 1. Materials and characterization

$Fe(NO_3)_3{\cdot}9H_2O$, $Sr(NO_3)_2$ and dichloromethane were purchased from Merck Company. All the chemicals were used as received without further purifications. X-ray diffraction (XRD) patterns were recorded by a Philips X-ray diffractometer using Ni-filtered CuK_α radiation. A multiwave ultrasonic generator (Bandeline MS 73) equipped with a converter/transducer and titanium oscillator with a maximum power output of 130 W was used for the ultrasonic irradiation. Scanning electron microscopy (SEM) images were obtained using a LEO instrument (Model 1455VP). Prior to taking images, the samples were coated by a very thin layer of Pt (BAL-TEC SCD 005 sputter coater) to make the sample surface conductor obtain better contrast and prevent charge accumulation. Room temperature magnetic properties were investigated using an alternating gradient force magnetometer (AGFM) device (Meghnatis Daghigh Kavir Company) in an applied magnetic field sweeping between ±10000 Oe.

2. 2. Synthesis of $SrFe_{12}O_{19}$ nanoparticles

$Sr(NO_3)_2$(0.001 mol), $Fe(NO_3)_3{\cdot}9H_2O$ (0.012 mol) and CTAB (0.5 g) are dissolved in 100 mL of distilled water. NaOH solution (50 mL, 1 M) is then slowly added to the mentioned solution under ultrasonic waves (80 W) for 30 minutes. The brown precipitate is then centrifuged and rinsed with distilled water and left in an atmosphere environment to dry. The resulting brown powder is then calcinated at 900° C in an oven for 4 hours.

2. 3. Synthesis of PS-SrM nanocomposite

Polymer (0.8 g) is first dissolved in dichloromethane (10 ml). The SrM nanoparticles (0.2 g) are dispersed in dichloromethane (10 ml) by ultrasonic waves. The nanoparticles dispersion is then slowly added to the polymer solution. The new solution is then stirred for 6 hours.

3. Results and discussion

The XRD pattern of SrM nanoparticles is shown in Fig. 1. and is indexed as a pure hexagonal phase (space group: P63/mmc).The experimental values are very close to the literature (JCPDS No. 24-1207).The crystallite size measurements were carried out using the Scherrer equation, the estimated crystallite size of product is about 24 nm.

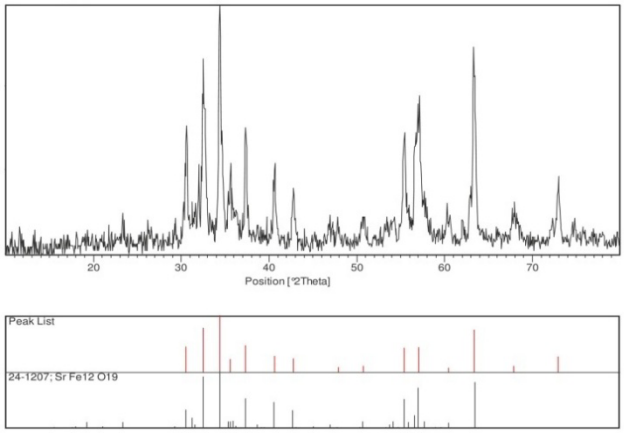

Fig. 1. XRD pattern of $SrFe_{12}O_{19}$ nanoparticles

The XRD patterns of ABS-SrM and PS-SrM nanocomposites are shown in Fig. 2 and 3 respectivelly.

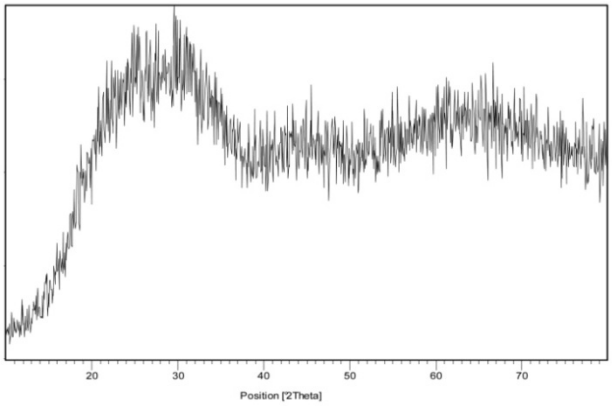

Fig. 2. XRD pattern of ABS-SrM nanocomposite

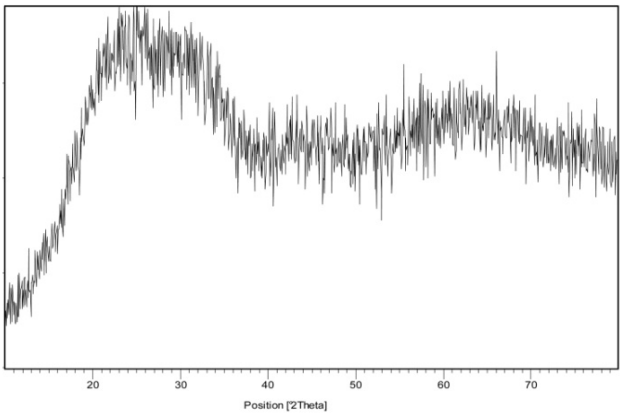

Fig. 3. XRD pattern of PS-SrM nanocomposite

Fig. 4 illustrates SEM image of the SrM nanoparticles that shows nanoparticles with average diameter of 30 nm. Fig. 5 depicts TEM image of the SrM nanoparticles that shows nanoparticles with mediocre diameter of 30 nm.

The room temperature magnetic properties of the samples were studied using an AGFM device. The SrM nanoparticles exhibit a hysteresis loop (Fig. 6). The appearance of a high coercive field in this loop correlates with the fact that there may be some particle aggregation, which behaves as a single large particle that may result in a multi-domain state. In such a case, the magnetization process may proceed by domain wall motion, which has a smaller coercive field than a re-magnetization process by coherent reversal.

In the best of our knowledge and based on our literature search, there are very few reports on hard magnetic polymeric nanocomposites. Therefore, we studied the magnetic interaction between the nanoparticles surrounded by polymeric chains. This interaction leads to a remarkable increase (from 5070 Oe to 5600 Oe) of nanoparticle coersivities relative to pure strontium ferrite nanoparticles. The hysteresis loops for ABS/SrM, PS/SrM, CA/SrM and PC/SrM are illustrated in Figs. 7-10 respectively.

In order to make 1g of magnetic nanocomposite, 0.2 g of strontium ferrite nanoparticles is added to 0.8 g of polymer. Thus, the nanocomposite magnetization (defined as the magnetic moment per unit volume) is about one fifth of that obtained for strontium ferrite nanoparticles.

The hysteresis loops for the polymer/strontium ferrite nanocomposites are practically the same as calculated originally by Stoner and Wohlfarth for an assembly of non-interacting single-domain particles

with uniaxial magnetic anisotropy, the assembly of which possesses a random orientation of the magnetic easy axes ($H_c \cong 0.5\ H_k$ where $H_k = 2K/M_s$ is the anisotropy field, K is the anisotropy energy and $M_r/M_s \cong 0.5$). This result is reproduced in many magnetic textbooks [15]. The origin of K may be magnetocrystalline anisotropy, shape or stress. Considering the data in Table 1, it is concluded that all the studied magnetic nanocomposites fulfill the requirements for such an analogy. A slight variation of coercive field and remanence values may be due to a non-uniformity of the ferrite powder or a different filling factor of the ferrite in the polymeric matrix. It can be concluded that the strontium ferrite particles in the nanocomposites are sufficiently distanced from each other in order to prevent their magnetic behavior be influenced by the stray fields of other particles; i.e., they are uncoupled (non-interacting).

The saturation magnetization of SrM nanoparticles is much higher than that obtained for the polymer/BaM nanocomposites. the nanocomposite magnetization (defined as the magnetic moment per unit volume) is much lower (about one fifth) than that obtained for strontium ferrite nanoparticles.

The results also indicate that forming the nanocomposite and distributing the magnetic nanoparticles into the polymer matrix leads to an increased coercivity. A possible explanation is the following: the magnetic moments of the nanoparticles are fixed by the surrounding polymer matrix chains so that a higher magnetic field is required for the alignment of the single domain nanoparticles in the field direction.

The coercivity of PC/SrM nanocomposites is also higher than that of the other polymer/SrM nanocomposites. Coercivity of magnetic nanocomposites depends on the magnetic nanoparticle distribution into the polymeric matrixes. Since these distributions differ from polymer to polymer, the coercivities also differ from one nanocomposite to the other, though the magnetic nanoparticles are similar (but in different distributions). The coercivity of ferrite nanoparticles distributed in the polymeric matrix is higher than pure nanoparticles.

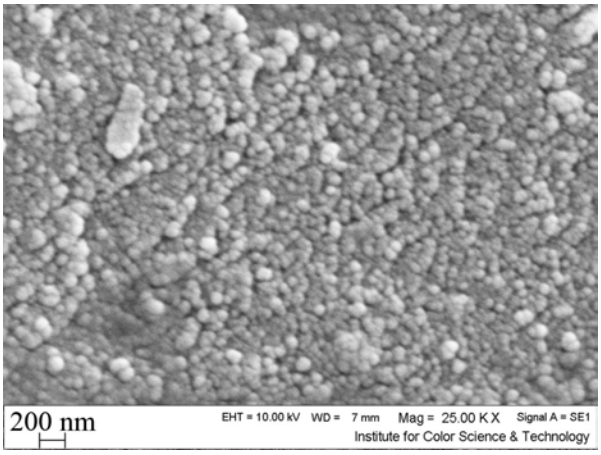

Fig. 4. SEM image of $SrFe_{12}O_{19}$ nanoparticles

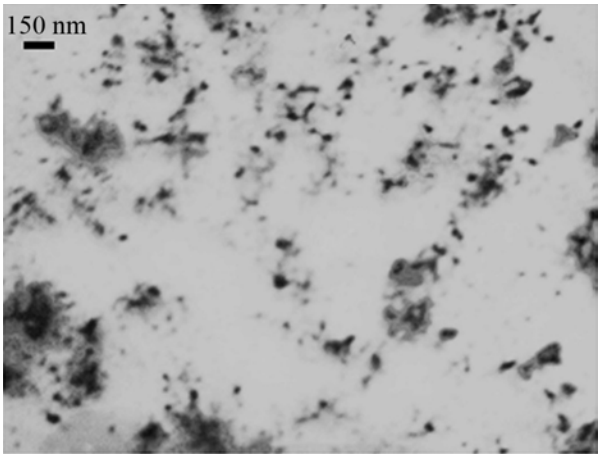

Fig. 5. TEM images of $SrFe_{12}O_{19}$ nanoparticles

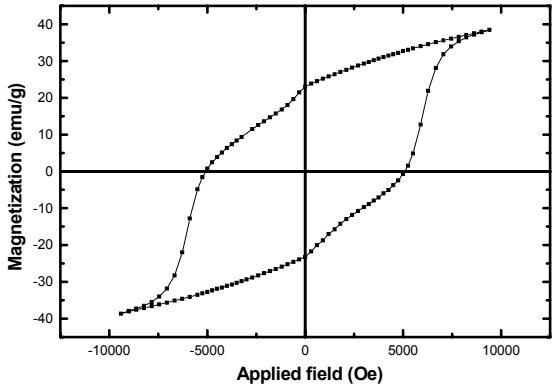

Fig. 6. Room temperature magnetization curves of $SrFe_{12}O_{19}$ nanoparticles.

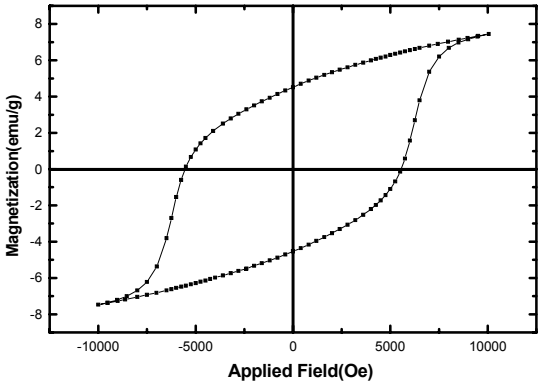

Fig. 9. Room temperature magnetization curve of PC-SrM nanocomposite . .

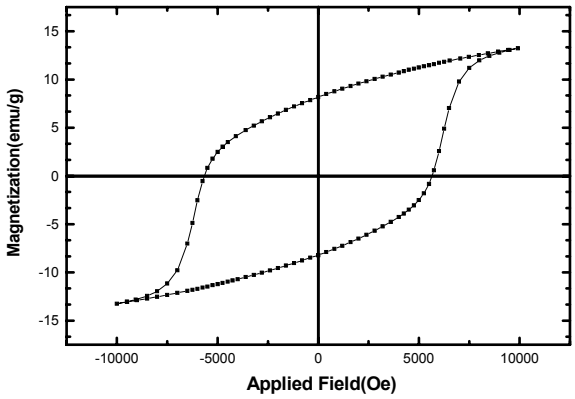

Fig. 7. .AGFM curve of PS-SrM nanocomposite

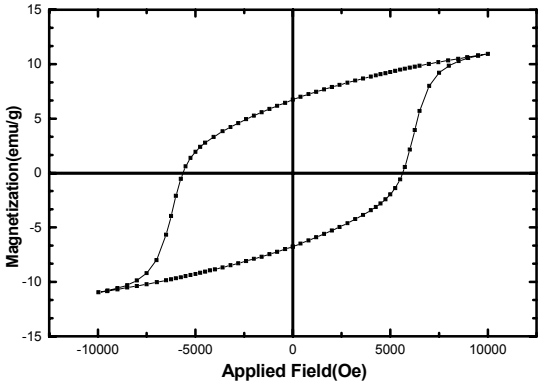

Fig. 10. AGFM curve of PSu-SrM nanocomposite.

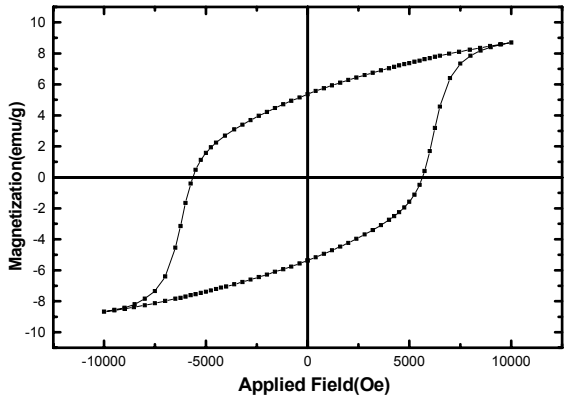

Fig. 8. .AGFM curve of ABS-SrM nanocomposite .

4. Conclusion

$SrFe_{12}O_{19}$ nanoparticles are synthesized by a simple sonochemical-assisted reaction. The $SrFe_{12}O_{19}$ nanoparticles exhibited ferromagnetic behavior with a saturation magnetization of 39 emu/g and a coercivity of 5070 Oe at room temperature. $SrFe_{12}O_{19}$ nanoparticles were then added to ABS, PS, PC and PSu polymeric matrixes to make magnetic nanocomposites. The nanocomposites were characterized by XRD and SEM spectroscopy. The distribution of $SrFe_{12}O_{19}$ nanoparticles into the polymeric matrixes substantially increases the coercivity. A maximum coercivity of 5600 Oe was

found for $SrFe_{12}O_{19}$distributed in the PSu matrix forming PSu/$SrFe_{12}O_{19}$ nanocomposite.

Acknowledgements

This work has been supported financially by Arak University Research Council (AURC) under the grant number of 90/10357. The authors acknowledge AURC for the financial support. The authors would also like to thank N. Nabiyouni for English assistance.

References

[1] D. Lisjak, M. Drofenik, J Eur Ceram Soc. 26, 3681 (2006).
[2] M. Pal, S. Bid, S.K. Pradhan, B.K. Nath, D. Das, D. Chakravorty, J Magn Magn Mater. 269, 42 (2004).
[3] K. Li, H. Gu, Q. Wei, China. Partic. 2, 41 (2004).
[4] V.K. Sankaranarayanan, Q.A. Pankhurst, D.P.E. Dickson, C.E. Johnson, J. Magn. Magn. Mater. 120, 73 (1993).
[5] K. V. P. M. Shafi, I. Felner, Y. Mastai, A. Gedanken, J. Phys. Chem. B 103, 3358 (1999).
[6] E. Matuevic, J Colloid Interf Sci. 117, 593 (1987).
[7] Z. Yang , C.S. Wang, X.H. Li, H.X. Zeng, Mater Sci Eng B-Adv. 90, 142 (2002).
[8] Z. Durmus, B. Unal, M.S. Toprak, H. Sozeri, A. Baykal, Polyhedron. 30, 1349 (2011).
[9] U. Topal, H. Ozkan, H. Sozeri, J Magn Magn Mater. 284, 416 (2004).
[10] Z. Durmus, H. Kavas, H. Sozeri, M. S. Toprak, A. Aslan, A. Baykal, J Supercond Nov Magn. 25, 1185 (2012).
[11] Z. Durmus, B. Unal, M.S. Toprak, A. Aslan, A. Baykal, Physica. B 406, 2298 (2011).
[12] B. Unal, Z. Durmus, A. Baykal, M.S. Toprak, H. Sozeri, A. Bozkurt, J Alloy Compd. 509, 8199 (2011)
[13] D. Ghanbari, M.Salavati-Niasari, M. Sabet, J Clust Sci. 23, 1081 (2012).
[14] M. Esmaeili-Zare, M. Salavati-Niasari, A. Sobhani, Ultrason Sonochem.19, 1079 (2012)
[15] J. Coey, Magnetism and Magnetic Materials, Cambridge University Press, 2010.